

A Facile Oxygen-17 NMR Method to Determine Effective Viscosity in Dilute, Molecularly Crowded and Confined Aqueous Media

Nasrollah Rezaei-Ghaleh,^{*a,b} Francesca Munari,^c Stefan Becker,^b Michael Assfalg^c and Christian Griesinger^b

^a Department of Neurology, University Medical Center Göttingen, Göttingen, Germany

^b Department for NMR-based Structural Biology, Max Planck Institute for Biophysical Chemistry, Göttingen, Germany

^c Department of Biotechnology, University of Verona, Verona, Italy

EXPERIMENTAL SECTION

Materials

Ficoll 70 and 1,1,1,3,3,3-Hexafluoro-2-propanol (HFIP) were obtained from Sigma-Aldrich. Sucrose was from Merck and agarose from Invitrogen. Deionized Milli-Q water was used for all aqueous solutions.

The Ile-Phe dipeptide was purchased from Bachem (product number 4001668.0001) and used without further purification. The peptide was dissolved in HFIP at 200 mg/mL concentration.¹ For gel formation, the stock solution of the peptide was diluted to 30 mg/mL by adding heated water containing 10% D₂O.^{1,2} The sample was then transferred to a 3-mm NMR tube before it formed the gel.

The FG-based peptide (sequence: Acetyl-GGGGGGLFGGNNNQQTNPTA-Amid) capped at both N- and C-termini, was obtained from Peptide Specialty Laboratory (PSL, Heidelberg, Germany). For gel formation, peptide solutions in 50 mM potassium phosphate (pH 6.8) were prepared at three concentrations, 1.6, 8 and 20 mM, and immediately transferred to 3-mm NMR tubes. The gel formation was evident in the samples leftover in the Eppendorf tube.

¹⁵N, ¹³C-labeled ubiquitin and heterotrimeric G protein beta subunit 3 (GB3) were prepared recombinantly, as described in references^{3,4}.

¹⁷O NMR

¹⁷O nucleus has spin quantum number I of 5/2 and natural abundance of 0.037%. The quadrupole moment (Q) of ¹⁷O is -2.63 fm², which interacts with the electric field gradient present at the site of ¹⁷O nuclei.⁵ The quadrupolar interaction is anisotropic and therefore in the absence of rotational averaging leads to broad powder patterns in NMR spectra.⁶ In solution, the traceless quadrupolar interaction is entirely averaged out by fast unrestrained molecular reorientations and only indirectly contributes to relaxation processes.⁷ As the dominant relaxation mechanism of ¹⁷O, the quadrupolar interaction in general case leads to a three-exponential relaxation process.⁸ However, in the extreme narrowing regime, the terms related to two of these relaxation processes are cancelled and consequently a single-exponential relaxation is recovered.^{7,8}

¹⁷O NMR experiments were performed at a Bruker spectrometer with proton Larmor frequency of 400.13 MHz. The spectrometer was equipped with a room-temperature triple resonance broadband (TBO) probe, where for the ¹⁷O-detected experiments the inner coil of the probe was tuned and matched at ¹⁷O Larmor frequency of ~ 54.24 MHz. The temperature was controlled to ± 0.05 K using the Bruker VT unit calibrated using a standardized thermocouple. The NMR samples contained H₂O/D₂O at a ratio of 90%/10% (v/v), unless specified otherwise, and the deuteron signal was used for frequency locking. The NMR samples were prepared using deionized Millipore water and were degassed under N₂ gas for ~ 10

minutes before NMR measurements. To alleviate the problem of baseline distortions potentially caused by the transient response of the NMR probe, a relatively long pre-acquisition delay of 18 μ s was used. The ^{17}O spectra are shown using the frequency of H^2DO lock signal as the chemical shift reference (4.700 ppm).

The ^{17}O longitudinal relaxation rates (R_1) were measured through standard inversion-recovery (d_1 -180°- t -90°-acq) pulse sequence, where duration of recovery time, t , varied from 0.25 to 30 ms. A total of 21 recovery data points were collected. A recycle delay (d_1) of 0.5 s was used. The data were fitted to a three-parameter single-exponential recovery function, as follows:

$$I = I_\infty(1 - 2be^{-R_1t}) \quad (\text{eq. S1})$$

where I_∞ represents signal intensity after complete recovery, R_1 is the longitudinal relaxation rate, and parameter b takes care of slight imperfections in the inversion pulse.

The rotational correlation time of water molecules (τ_{rot}) were calculated from ^{17}O R_1 rates through equation S2:

$$R_1 = \frac{3\pi^2}{10} \left(\frac{2I+3}{I^2(2I-1)} \right) \chi^2 \left(1 + \frac{\eta^2}{3} \right) \tau_{\text{rot}} \quad (\text{eq. S2})$$

where $I=5/2$ is the spin quantum number of ^{17}O , $\chi = \frac{e^2Qq_{zz}}{h}$ is quadrupole coupling constant (C_Q) and η is the asymmetry parameter, describing the deviation of electric field gradient tensor, q , from axial symmetry. This equation relies on the assumption of the extreme-narrowing regime, where $J(0)=J(\omega)=J(2\omega)$.⁷ This is a good approximation, when rotational correlation times are shorter than $1/(20\omega_0)$, i.e. ~ 150 ps, a condition which holds for bulk water (H_2^{17}O or D_2^{17}O) molecules in all our experimental conditions. It is notable that the obtained τ_{rot} corresponds to the rotational correlation time of the principal axis of the electric field gradient tensor at the ^{17}O nucleus of water molecules, which is an out-of-plane vector orthogonal to O-H bonds, and therefore does not necessarily represent rotational correlation times around other axes of water molecules.⁹

To find an empirical relation between the ^{17}O R_1 rates of water, which in the extreme narrowing regime are proportional to the τ_{rot} of water molecules, and solution viscosity in glycerol-water mixtures, polynomial equations of degrees 1, 2 and 3 were tried. At 298 K, the fit to a quadratic equation was significantly better than a linear equation (p-value < 0.001), but a cubic equation did not show a significant improvement in the fit when compared to a quadratic equation (p-value ~ 0.744). It is however important to note that the effective viscosity experienced by relatively large biomolecules is a collective property determined through a complex function of the properties of individual water molecules, e.g. their τ_{rot} . Consequently, the quadratic equation (equation 1 in the main text) should be seen only as an empirical relation without implying any particular physical model or interpretation for the coefficients.

¹⁵N relaxation

¹⁵N relaxation experiments were performed at a Bruker spectrometer with a proton Larmor frequency of 599.9 MHz equipped with a cryogenic QCI probe. NMR samples contained 4 mM uniformly labelled ubiquitin or 3 mM GB3, buffered with 50 mM sodium phosphate and 100 mM sodium chloride at pH 6.5. The ¹⁵N/¹⁵N-¹H (CSA/DD) cross-correlated relaxation (*CCR*) rates were measured at 298 K, following a standard pulse sequence¹⁰, using relaxation delays of 40, 60, 80, 100 and 120 ms. The obtained *CCR* rates closely matched the rates measured through another pulse sequence,¹¹ where the use of four complementary experiments enabled cancelling errors due to pulse miscalibrations and uncontrolled attenuation factors. The residue-specific rotational correlation times (τ_c) were estimated from the *CCR* rates, using a ¹⁵N CSA magnitude of -160 ppm and an angle of 17° between the principal axis of the ¹⁵N CSA tensor and internuclear N-H vectors.¹²

The ¹⁵N longitudinal (R_1) and transverse (R_2) relaxation rates of 0.37 mM ubiquitin in dilute and crowded solutions (200 mg/mL Ficoll 70 or 200 mg/mL sucrose) solutions were obtained from reference¹³. The residue-specific τ_c values were calculated from R_2/R_1 ratios,¹⁴ using an in-house MATLAB script (see below, page S14).

Hydrodynamic calculations

To predict viscosity in highly concentrated protein solutions, hydrodynamic calculations were performed using HYDROPRO 10,¹⁵ which provide hydrodynamic parameters of proteins at infinite dilution using a bead model of their known atomistic structures as the starting point. The PDB entries of 1UBQ (ubiquitin) and 1P7F (GB3) were used for hydrodynamic calculations.^{16, 17} The bead models were constructed using an atomic effective radius (AER) of 2.5 to 3.0 Å.¹⁵ The errors in hydrodynamic calculations were estimated through standard deviation of the obtained results over the range of AER values. Taking the intrinsic viscosity-related radii from HYDROPRO 10 results, the volume occupancy (ϕ) was calculated, then, the relative viscosity (η/η_0) was predicted using the Guth-Gold-Simha equation,¹⁸

$$\frac{\eta}{\eta_0} = 1 + 2.5\phi + 14.1\phi^2 \text{ (eq. S3)}$$

where η_0 is the bulk viscosity. Equation 3 reduces to the Einstein equation,¹⁹

$$\frac{\eta}{\eta_0} = 1 + 2.5\phi \quad \text{(eq. S4)}$$

at sufficiently small ϕ values. The calculated ϕ values were 5.2±0.2% in 4 mM ubiquitin and 2.7±0.1% in 3 mM GB3 solutions. Using the Guth-Gold-Simha equation (eq. S3), the increase in solution viscosity was predicted to be 17±1 % for 4 mM ubiquitin and ~ 8% for 3 mM GB3 protein.

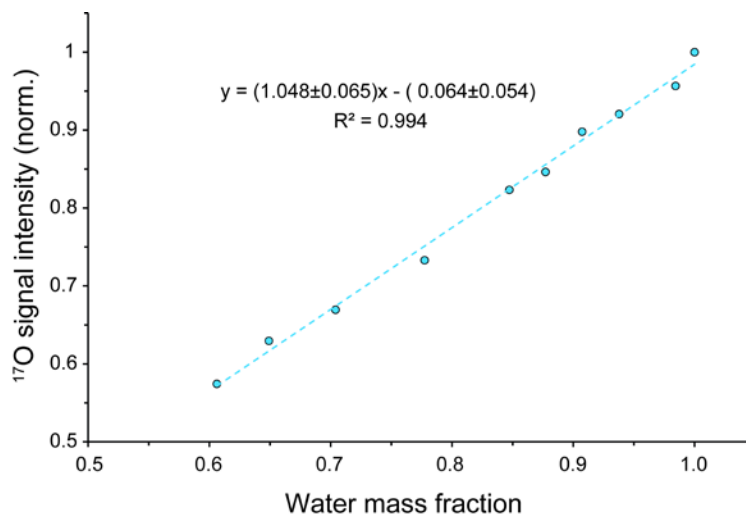


Figure S1. In 1D ¹⁷O NMR spectra of water-glycerol mixtures, obtained through pulse-acquire experiments, the integrated intensity of the H₂¹⁷O signals changes in line with water content of the measured samples. The signal intensities are normalized to the value obtained at 0% glycerol (i.e. 100% water). A good linear relation with a slope of 1.048 (95% CI: 0.983-1.113) is observed.

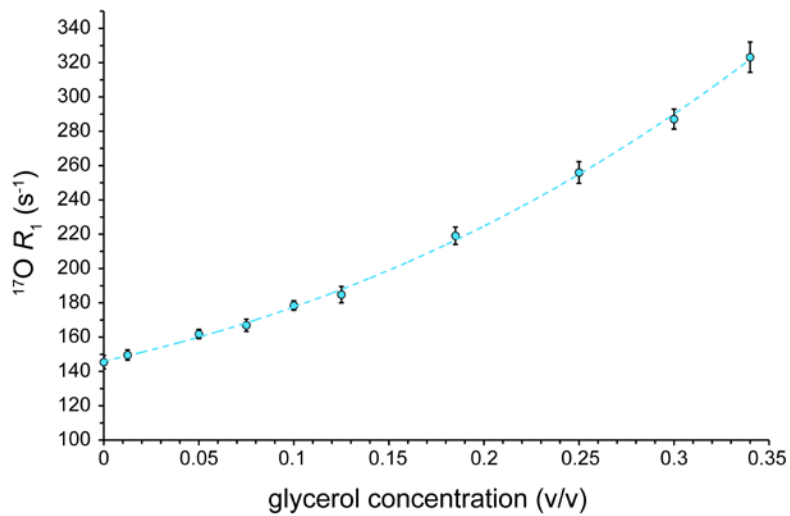


Figure S2. ^{17}O longitudinal relaxation rate (R_1) of water in water-glycerol mixtures, measured through inversion-recovery experiments, as a function of glycerol (v/v) concentration.

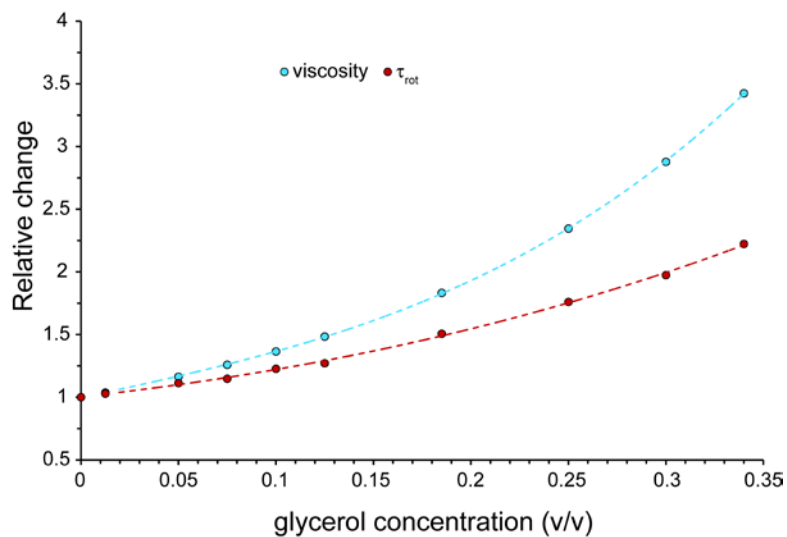


Figure S3. Upon increasing glycerol concentration, relative changes in solution viscosity and rotational correlation time (τ_{rot}) of water molecules calculated from ^{17}O R_1 rates are compared. The solution viscosity is affected by glycerol addition more prominently than the τ_{rot} of water molecules.

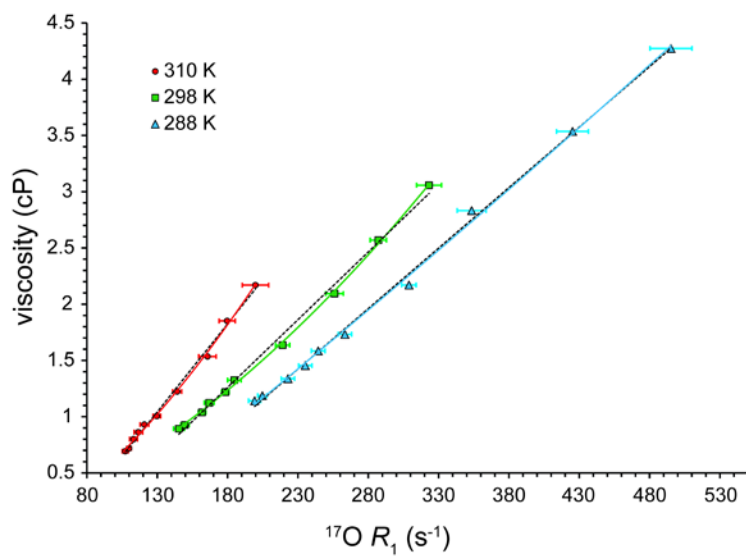


Figure S4. Relation between viscosity of water-glycerol mixtures and the ^{17}O longitudinal relaxation rate (R_1) of water, obtained at three temperatures of 288, 298 and 310 K. The linear (black dashed lines) and quadratic (solid lines) fits are shown.

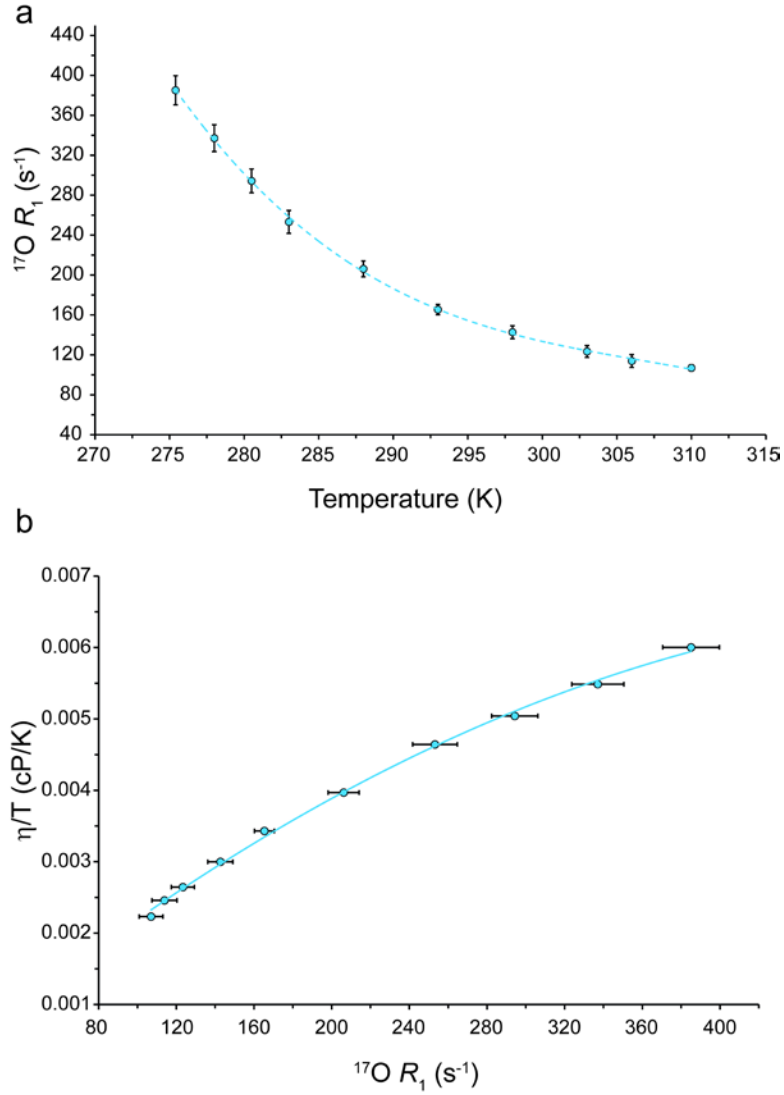


Figure S5. (a) Temperature-dependence of ^{17}O longitudinal relaxation rate (R_1) of water, showing the expected decrease of $^{17}\text{O } R_1$ of water upon increasing temperature from 275.5 to 310 K. (b) The relation between viscosity/temperature ratio (η/T) and $^{17}\text{O } R_1$ of water exhibits a deviation from linearity. The quadratic fit corresponding to equation, $\frac{\eta}{T} \left(\frac{\text{cP}}{\text{K}} \right) = -2.037 * 10^{-8} * (R_1)^2 + 2.303 * 10^{-5} * R_1 + 9.305 * 10^{-5}$, is shown as solid line.

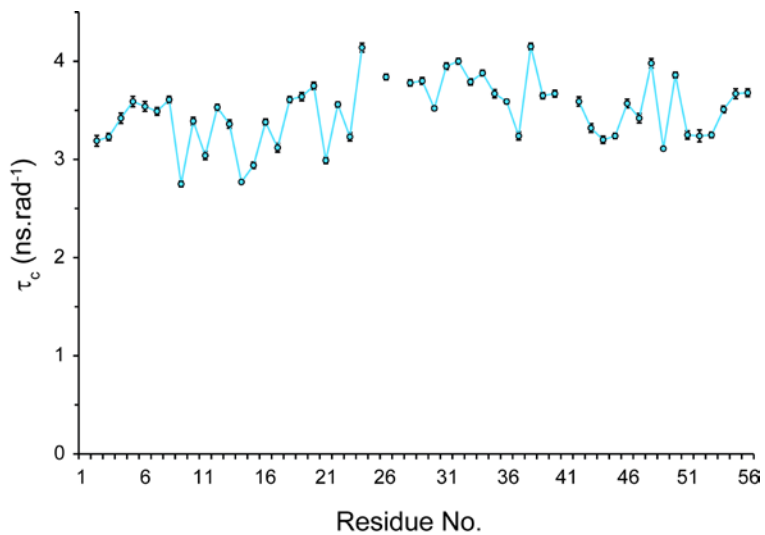


Figure S6. Residue-specific rotational correlation times (τ_c) of GB3 at 3 mM concentration, derived from $^{15}\text{N}/^{15}\text{N}-^1\text{H}$ CSA/DD CCR rates measured at 298 K. For the CCR-based calculation of τ_c , the Lipari-Szabo's N-H squared order parameters (S^2) of GB3 were taken from literature.²⁰ Little variation (less than $0.02 \text{ ns}\cdot\text{rad}^{-1}$) was observed when rotational correlation time of internal motion (τ_i) ranged between 40 and 100 ps.

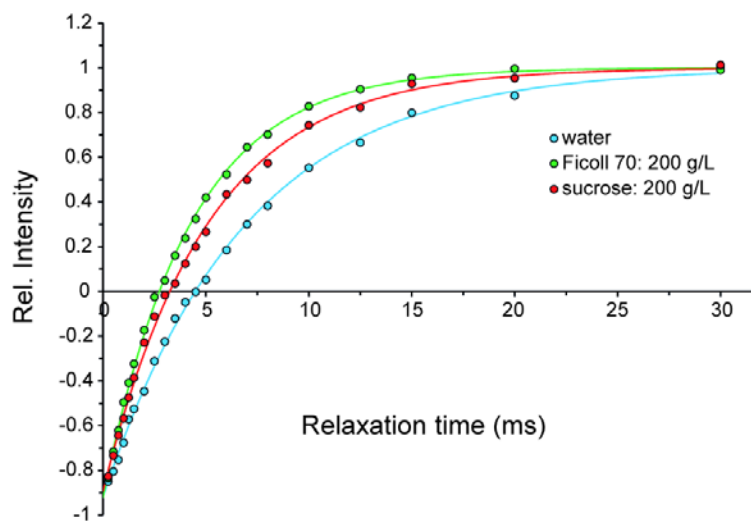


Figure S7. ^{17}O longitudinal relaxation rate (R_1) of water in dilute and crowded (200 g/L Ficoll 70 or sucrose) media, measured through inversion-recovery experiments. Relative intensities of water ^{17}O signals are shown as a function of recovery time. Faster recovery is observed in sucrose and particularly Ficoll solutions, compared to water.

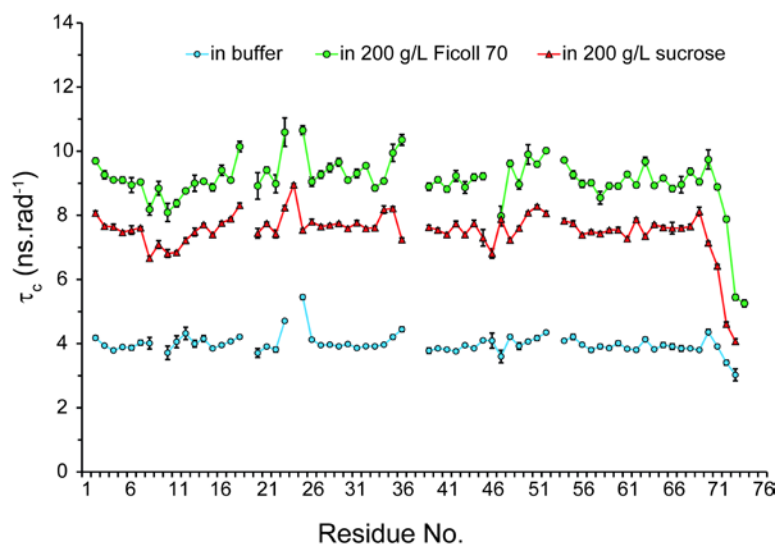


Figure S8. Residue-specific rotational correlation times (τ_c) of ubiquitin, derived from ^{15}N R_2/R_1 ratios. The ^{15}N R_1 and R_2 rates are taken from reference ¹³. The τ_c values are shown for 0.37 mM ubiquitin in buffer, in 200 g/L sucrose and 200 g/L Ficoll 70 concentrations.

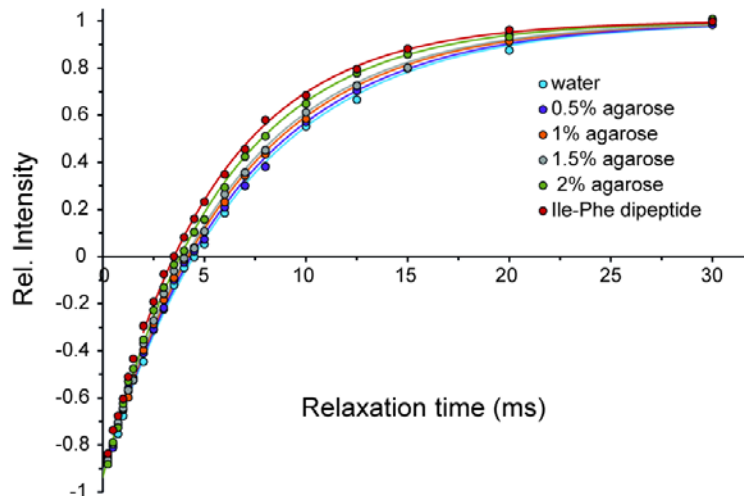


Figure S9. Water dynamics in the confined media of biological hydrogels, as probed by ^{17}O longitudinal relaxation rate (R_1) of water. ^{17}O R_1 of water in agarose and Ile-Phe hydrogels were measured through inversion-recovery experiments. Relative intensities of water ^{17}O signals are shown as a function of recovery time. Intensity recovery becomes faster when agarose concentration is increased.

```

clc
clear all

%% INTRODUCTION
% disp('AUTHOR: N. Rezaei-Ghaleh (Hessam): nare@nmr.mpibpc.mpg.de')
disp('This program is to derive tauc from 15N R2/R1 ratio')
% disp('Based on Biochemistry 1989, 28(23): 8972-8979')
% disp(' ')
disp('Check field (Bh), rhn and csan parameters and the input .xlsx file ')
disp('Set n as the number of residues you have in the input file ')
% disp('Results will be written in the output.txt file; There will be 8 tau-c solutions per
residue, take the physically meaningful values.')
```



```

%% INPUTS %%
n = 73 ; % No. of residues
Bh = 600.13 ; % (MHz)
rhn = 1.02*10^-10 ; % (* m *)
% rhc = 1.106*10^-10 ; % (* m *)
csan = -160*10^-6; % CSA of 15N
R = xlsread('input.xlsx','B3:B75'); % R2/R1 ratio taken from the input .xlsx file, column B
%-----%
```



```

Gn = -2.712*10^7 ; % (* rad/(T s) *)
Gh = 2.6752*10^8 ; % (* rad/(T s) *)
%Gc = 6.728*10^7 ; % (* rad/(T s) *)
h=6.62606896*10^-34 ; % J.s
u0=4*pi*10^-7 ; % (* uo = Bo/H; H = A/m; uo = T m/A *)
B0=Bh*10^6*2*pi/Gh ; % (in Tesla)
dd= (u0/4/pi)^2*(h/2/pi)^2*Gn^2*Gh^2/((rhn)^6)/(10^9);% dipolar coupling prefactor, scaled down
cc= csan^2*B0^2*Gn^2/3/(10^9); % csa prefactor, scaled down
Wh=Bh*10^6*2*pi ; % angular freq. of 1H
Wn=Wh*Gn/Gh ; % angular freq. of 15N
```



```

for j=1:1:n ;

%% OPENING the file to write down the results
fid=fopen('output.txt','a+');

%% Solve the nonlinear equation f(t)=0
% Define x (tauc)
syms x
f=((dd/8)*(4*x+(x/(1+((Wh-
Wn)*x)^2))+3*(x/(1+((Wn)*x)^2))+6*(x/(1+((Wh)*x)^2))+6*(x/(1+((Wh+Wn)*x)^2)))+(cc/6)*(3*(x/(1+((W
n)*x)^2))+4*(x)))/((dd/4)*(x/(1+((Wh-
Wn)*x)^2))+3*(x/(1+((Wn)*x)^2))+6*(x/(1+((Wh+Wn)*x)^2)))+(cc)*((x/(1+(Wn*x)^2)))) - R(j) ;

%% DISPLAYING INPUTS

disp('INPUTS')

func=[' The equation to be solved is ' char(f), '=0'];
disp(func)
disp(' ')

% solving the equation
soln=solve(f,x);
solnvalue=double(soln);

disp('OUTPUTS')

fprintf(fid, '\nThe residue# %f ', j) ;
for i=1:length(solnvalue)
fprintf('\nThe solution# %g is %g', i,solnvalue(i))
fprintf(fid, '\nThe solution# %g is %g', i,solnvalue(i));
end

end
fclose(fid) ;
disp(' ')

```

References

1. N. S. de Groot, T. Parella, F. X. Aviles, J. Vendrell and S. Ventura, *Biophys. J.*, 2007, **92**, 1732-1741.
2. S. Mamone and S. Glogglar, *Phys. Chem. Chem. Phys.*, 2018, **20**, 22463-22467.
3. M. Renatus, S. G. Parrado, A. D'Arcy, U. Eidhoff, B. Gerhartz, U. Hassiepen, B. Pierrat, R. Riedl, D. Vinzenz, S. Worpenberg and M. Kroemer, *Structure*, 2006, **14**, 1293-1302.
4. A. M. Gronenborn, D. R. Filpula, N. Z. Essig, A. Achari, M. Whitlow, P. T. Wingfield and G. M. Clore, *Science*, 1991, **253**, 657-661.
5. I. P. Gerothanassis, *Prog. Nucl. Magn. Reson. Spectrosc.*, 2010, **56**, 95-197.
6. M. J. Duer, *Introduction to Solid-State NMR Spectroscopy*, Blackwell, 2004.
7. A. Abragam, *The Principles of Nuclear Magnetism*, Oxford University Press, 1961.
8. I. P. Gerothanassis and C. G. Tsanaktsidis, *Conc. Magn. Reson.*, 1995, **8**, 63-74.
9. J. Ropp, C. Lawrence, T. C. Farrar and J. L. Skinner, *J. Am. Chem. Soc.*, 2001, **123**, 8047-8052.
10. N. Tjandra, A. Szabo and A. Bax, *J. Am. Chem. Soc.*, 1996, **118**, 6986-6991.
11. P. Pelupessy, G. M. Espallargas and G. Bodenhausen, *J. Magn. Reson.*, 2003, **161**, 258-264.
12. D. Fushman and D. Cowburn, *J. Am. Chem. Soc.*, 1998, **120**, 7109-7110.
13. F. Munari, A. Bortot, S. Zanzoni, M. D'Onofrio, D. Fushman and M. Assfalg, *FEBS Lett.*, 2017, **591**, 979-990.
14. L. E. Kay, D. A. Torchia and A. Bax, *Biochemistry*, 1989, **28**, 8972-8979.
15. A. Ortega, D. Amoros and J. Garcia de la Torre, *Biophys. J.*, 2011, **101**, 892-898.
16. S. Vijaykumar, C. E. Bugg and W. J. Cook, *J. Mol. Biol.*, 1987, **194**, 531-544.
17. T. S. Ulmer, B. E. Ramirez, F. Delaglio and A. Bax, *J. Am. Chem. Soc.*, 2003, **125**, 9179-9191.
18. E. Guth and R. Simha, *Kolloid Z.*, 1936, **74**, 266-275.
19. A. Einstein, *Ann. Phys.*, 1906, **19**, 289-306.
20. J. B. Hall and D. Fushman, *J. Biomol. NMR*, 2003, **27**, 261-275.